Atomic-scale study of the nonmelting, wetting, and freezing behavior of KCl(100)

A. Zaoui* and W. Sekkal[†]

Condensed Matter Group, International Center for Theoretical Physics, Strada Costiera 11, 34000 Trieste, Italy

The objective of this work is to study the thermodynamic properties of the KCl(100) surface by means of Molecular Dynamics (MD) simulation based on the Fumi-Tosi potential. The reliability of this potential model was tested to be quite accurate from the calculated bulk melting temperature T_m. The latter quantity was derived from the coexistence procedure of both solid and liquid states. After this preliminary study, the surface (100) of KCl was heated up to the bulk melting temperature and overheated until $T_m + 243$ K. As wetting and melting are thermodynamically linked, we have also investigated the wetting behavior from the calculation of the angular contact between a liquid nanodroplet and the nonmelting surface of KCl. Our simulation results give an angle of 47° in fairly good agreement with the experimental data (49°), which confirm the nonmelting behavior of the surface. It appears, however, that the thermodynamic way followed by the surface under the freezing process is not the same while heating. The calculated freezing temperature value corresponds to $T_m + 215$ K. This predictive phenomenon is explained by the important difference between the molar fraction of the liquid and the solid sates.

I. INTRODUCTION

Surface melting was suggested as a possible mechanism for the onset of the bulk melting long ago. In the nineteenth century, Faraday made some original observations on possible surface melting of ice.[1] Qualitative interpretations were given much later,[2,3] and a clear experimental characterization has been given previously. Frenken and van der Veen[4,5] have first studied microscopically the surface melting of Pb(110) with ion-shadowing and blocking measurements which are sensitive to the formation of small liquid films at the surface. It was shown that the surface starts to disorder gradually at $T = 450$ K and that the thickness l of the liquid film diverges logarithmically approaching T_m. A similar study was done for Al(110) by van der Gon *et al.*[6] who found again a logarithmic growth of l. Surface melting can be regarded as a case of wetting of solid by its own melt. This phenomenon is characterized, at temperatures near but below the bulk melting point T_m, by the existence of a disordered and mobile film that wets the solid-vapor interface. The thickness of this film diverges as T_m is approached.

The problem of surface nonmelting has attracted the attention of several scientists during recent years.[7–14] Such a phenomenon became increasingly known especially for some metals. This appears in a specific orientation of the surface, which strongly depends on the surface energy of the given system. Several investigations have been paid, both theoretically and experimentally, to the thermodynamic properties of metal surfaces at high temperatures.[15–21] The main contribution and the novelty of the present work lies in the study of the surface of an ionic solid, KCl, which poses several challenges arising from the long-range Coulomb forces. Experimental studies have been done for KCl (Ref. 22) in order to measure the contact angle and to see the surface morphology of this compound under temperature. However, no theoretical studies of the high temperature of KCl surfaces have been explored so far.

The aim of this contribution is to study the thermodynamic properties of the KCl(100) surface from the melting/nonmelting side and for the opposite effect, i.e., the freezing behavior when cooling the overheated surface. To this end we will use a molecular dynamics method based on the two body potential of Fumi-Tosi,[23] which is the most appropriate for such a system. We will, first, determine the bulk melting temperature by means of the phase coexistence technique. This method was successfully used for simpler case of metals where phase diagram boundaries may be applied without excessive computational burden. In the present work, we are considering its first application to an ionic solid. As melting and wetting are closely linked thermodynamically, we will investigate the angular contact between a liquid droplet and the overheated surface as well as the freezing effect. In the following, we will describe the method used in Sec. II. The results are given and discussed in Sec. III. Section IV is the conclusion.

II. METHOD

For solid and liquid phases of alkali halides, we shall take as our "good first guess" potentials which consist of Coulombic terms and short range repulsive terms, for which the Born-Mayer (exponential) form will be assumed, supplemented by Van der Waals attractive terms. These pair potentials, first used by Huggins and Mayer may be written as

$$\phi_{ij}(r) = Z_i Z_j \frac{e^2}{r} + b \exp[B(\alpha_{ij} - r)] + \frac{C_{ij}}{r^6} + \frac{D_{ij}}{r^8}, \quad (1)$$

where i and j can be either $+$ or $-$, Z_i and Z_j are ± 1 if the system is assumed to be fully ionic and dipole-dipole and dipole-quadrupole terms are included. In this work, we employ this model to describe the interactions in our system based on the Born-Mayer-Huggins potential as parameterized by Fumi and Tosi.[23,24] The Coulomb long-range interactions were treated by the standard three-dimensional Ewald method.[25,26] The convergence parameters for the

TABLE I. Parameters of the pair potentials for KCl.

	α 10^{-8} cm	C 10^{-60} erg cm^6	10^{-76} erg cm^8
+ +	2.923	24.3	24.0
+ −	3.048	48.0	73.0
− −	3.170	124.5	250.0

Ewald summations were chosen in order to converge the real and reciprocal space sums to a given tolerance (10^{-5} Hartree per atom). The parameters α_{ij}, C_{ij}, and D_{ij} are given in Table I; $b=0.338\times10^{-12}$ erg and $B=2.97\times10^8$ cm^{-1}.

III. RESULTS AND DISCUSSIONS

A. Bulk melting properties

In order to study surface melting/nonmelting, it is important to determine precisely the bulk melting point for the potential used. This was a difficult problem for a long time due to hysteresis effect near the first-order transition: simulated crystals with periodic boundary conditions can be overheated to temperatures much higher than the equilibrium melting point. An appropriate technique was developed[7,27] by simulating the coexistence of solid and liquid phases, and then determine the coexistence through lack of motion of the solid-liquid interfaces. The melting point is the one for which the two states remain unchanged. This technique is suitable for both experimental and theoretical studies and it has been applied widely and successfully for metals,[7,28] which prompted us to use it for an ionic system with long-range forces.

For the technical procedure, we have chosen in the same box two equivalent parts of 12 solid layers and 12 liquid layers (3456 atoms of K and 3456 atoms of Cl). The liquid part was obtained by heating the layers over the experimental melting point by keeping the solid layers under a temperature considerably lower than the experimental melting point. Each part was kept unchanged when acting on the other one. T_m is estimated by performing several simulations at constant energy with various values for the total energy E. When E is chosen above the total energy, which corresponds to T_m, the system will be out of equilibrium and will tend to melt some of the solid part; while in the opposite case, some of the liquid will solidify. In the former case T_m will decrease as latent heat is absorbed from the kinetic energy, while in the latter case latent heat is released and T will increase. To ensure a sufficient relaxation of the system, we have used a long time of simulation (~0.5 ns).

In Fig. 1, we show the final configuration after equilibrating the system for $T_m=1132\pm13$ K for which there is a coexistence between the solid and the liquid regions. This value is in good agreement with the experimental findings (1050–1220 K, Ref. 29) which confirms the reliability of our potential model. We notice that the finite-size effects will not affect significantly T_m since we have used large systems with large sizes and the obtained error is only about 2%, i.e., less than our estimated one.
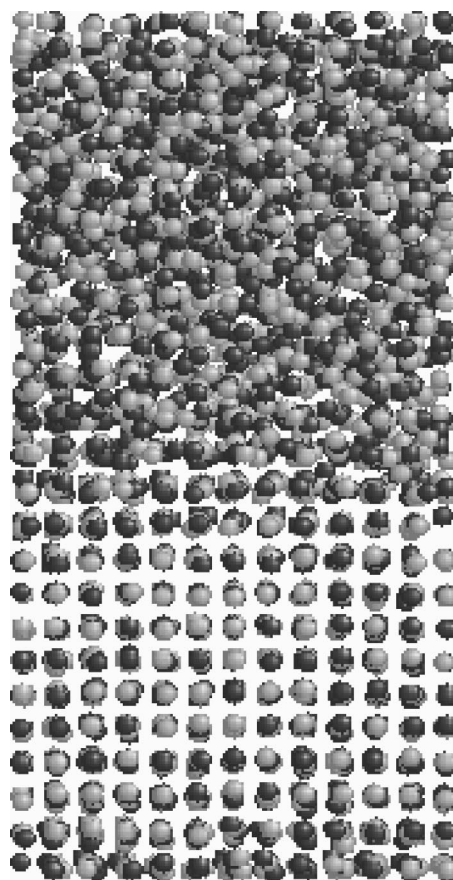

FIG. 1. Coexistence between solid and liquid at the bulk melting temperature.

B. Nonmelting behavior of KCl(100)

A 24-layer slab with three rigid bottom layers, one free surface, 224 atoms per layer, an x-y periodic boundary conditions was studied as a function of temperature. We use a canonical ensemble (NVT) for which we follow the temperature evolution by a step of 1 K which corresponds to the error bar of our results. As T_m was reached and crossed, the surface remained crystalline (metastable), up to a large temperature $T_i=T_m+243$ K ($T=1375$ K), even for very long runs (2 ns). In Fig. 2, we present a top view of our slab at different temperatures, below the bulk melting temperature [$T=1100$ K, see Fig. 2(a)] and gradually up to the surface melting {$T=1200$ K [Fig. 2(b)], 1375 K [Fig. 2(c)], 1400 K [Fig. 2(d)]}, where in the last case ($T=1400$ K) the surface shows a liquidlike structure. This behavior can be analyzed from the density profile as presented in Fig. 3. At $T=1200$ K, the surface is still ordered and the profile shows oscillations corresponding to the crystal planes; while at $T=1400$ K, the system is liquefied except the bottom where we have rigid planes. The melting/nonmelting surface is strongly related to the surface free energy of the various isolated interfaces γ_{SL}, γ_{LV}, γ_{SV} (S, L, and V indicate surface, liquid, and vacuum, respectively). In fact when the excess free energy $\Delta\gamma_\infty=\gamma_{SL}+\gamma_{LV}-\gamma_{SV}$ is negative, the state with a liquid film at the top is thermodynamically stable. This is the case, for instance, of Al (110),[32] Ni (110),[33] and Cu (110).[34]
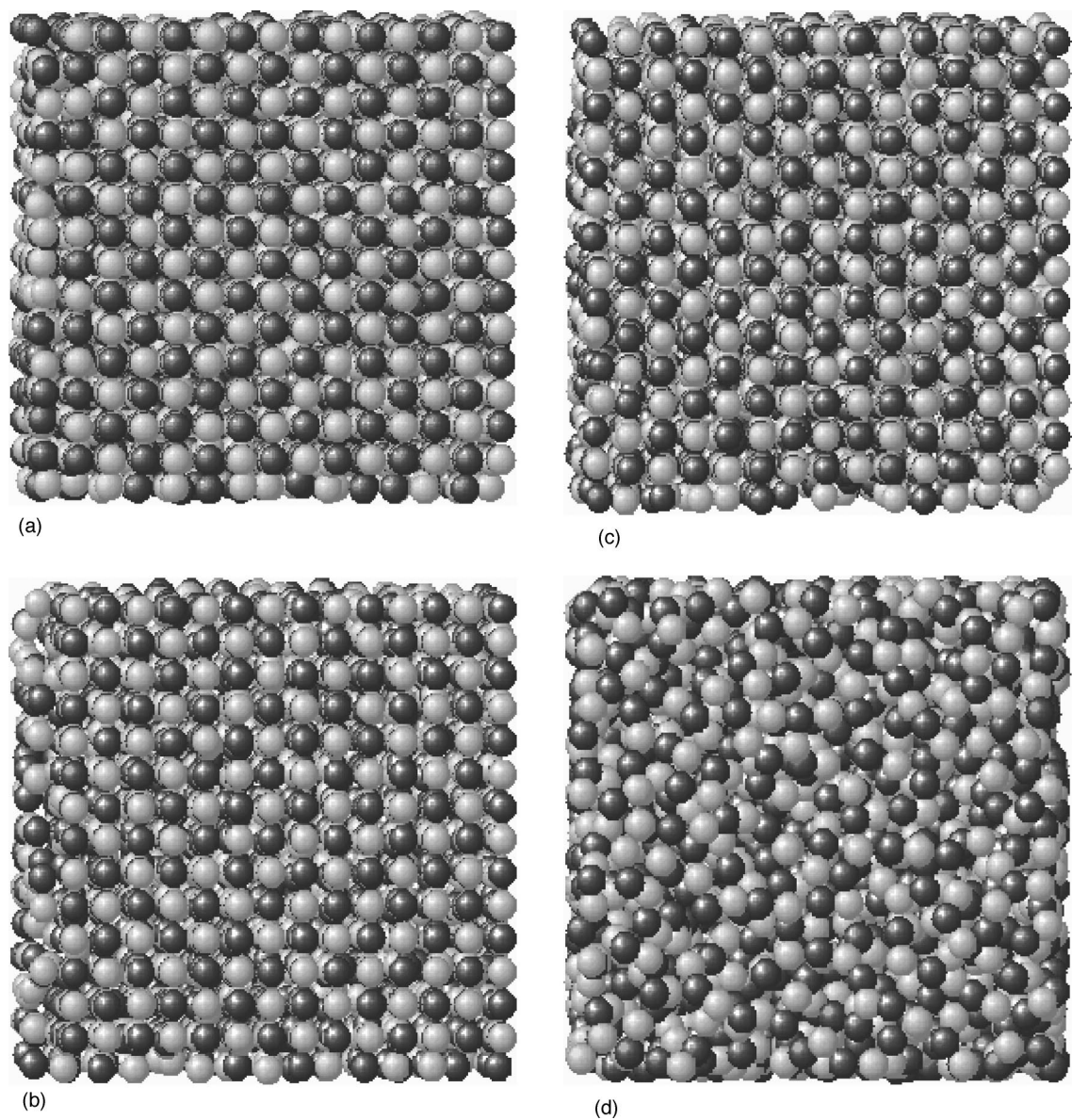
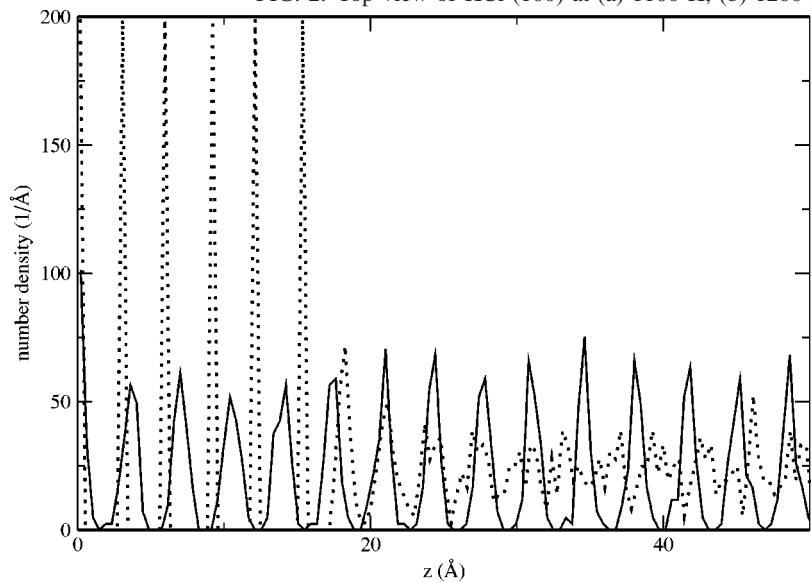FIG. 2. Top view of KCl (100) at (a) 1100 K, (b) 1200 K, (c) 1375 K, and (d) 1400 K.

FIG. 3. Calculated density profile of the KCl (100) at 1200 K (solid line) and at 1400 K (dashed line).
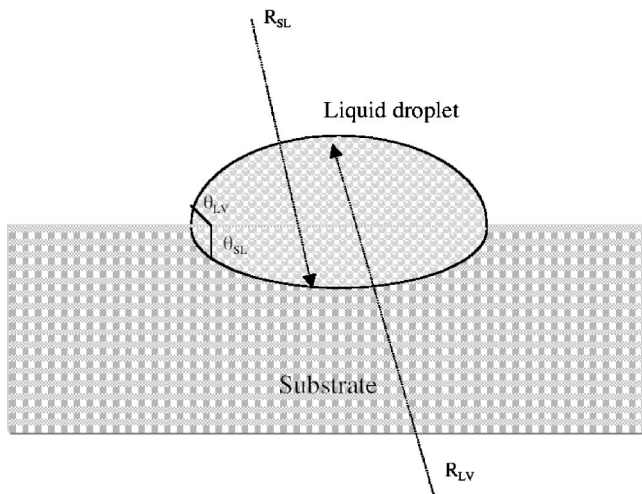
FIG. 4. A general geometry of the shape of a drop melt onto a nonmelting surface of the same material.

Moreover, it is important to notice that γ_{SV} and γ_{SL} depend on the crystalline orientation chosen. For example, simulations on Au (111),[35] Pb (111),[36] and Al (111) (Ref. 37) have shown that the opposite could also happen, i.e., certain surfaces may exhibit nonmelting behavior up to and even above bulk melting. This happen when $\Delta\gamma_\infty$ is positive, which is the case of KCl (100) where $\Delta\gamma_\infty = 35.2$ erg cm^2.

Below the melting temperature the surface atoms rearrange to compensate the lack of bonds compared to the bulk. This might bring, e.g., to a contraction, or dilatation, of the inter-layer separation of the topmost crystal planes, without change of symmetry. The generic name for this is surface relaxation. It may also happen that surface atoms rearrange completely to form new bonds, for which the bulk terminated surface has a lot of dangling-bonds and hence their atoms like to approach each other to share electrons, neutralize the surface and lower the surface free energy. After the rearrangement, the surface atoms will form a 2D lattice with different periodicity or symmetry with respect to that of the bulk planes parallel to the surface. The reconstructed state is usually the most stable at a very low temperature. When the temperature of a reconstructed surface is raised, the balance between the energetic and the entropic contributions to the free energy will generally lead to a deconstruction, i.e., to the removal of the new order and periodicity established by the reconstruction.

Approaching further the melting point the surface atoms move more and more freely. In the case of melting surfaces, one observes the formation of a thin quasiliquid film at the surface, characterized by a finite amount of diffusion. Quantitatively the atoms in the quasiliquid film have a diffusion coefficient D smaller than in the liquid phase, but similar (10^{-5} cm^2 s^{-1}).[30] The motion is essentially intraplane, with only a small interplane diffusion. Moreover the density profiles of the quasiliquid part is not flat but structured along the surface normal, and shows oscillations induced by the vicinity of the solid part.[30] This is the early stage of the melting of surface and from the thermodynamic point of view is equivalent to the self-wetting of the solid by its own liquid. The
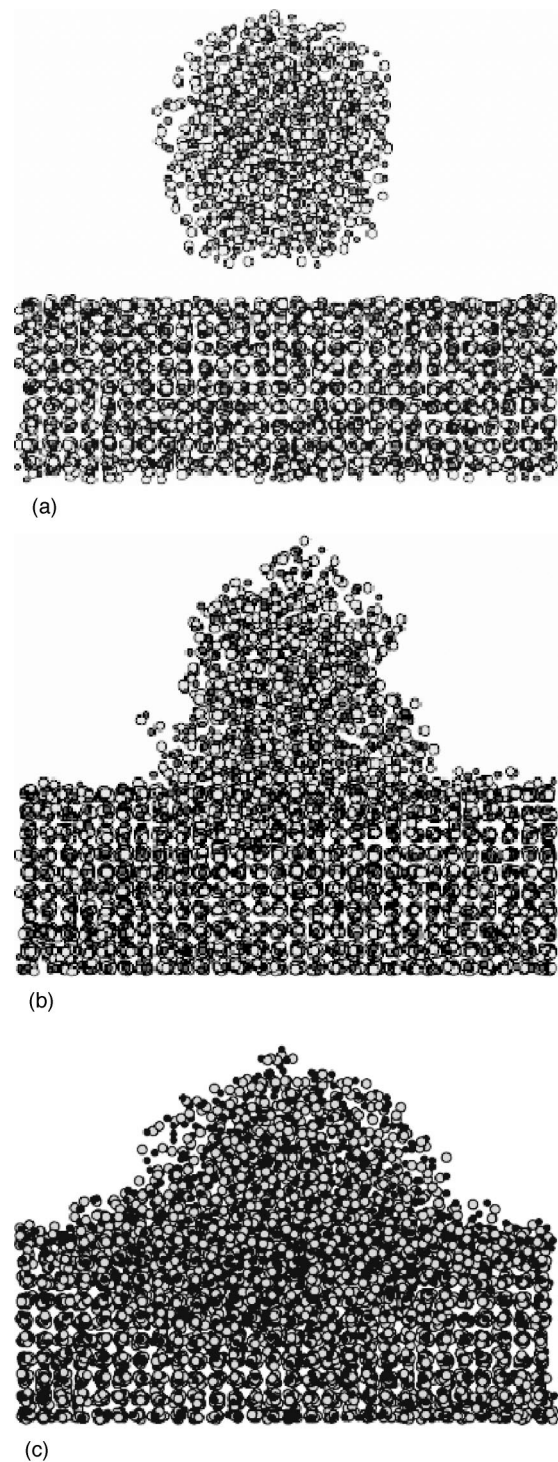

FIG. 5. Droplet of KCl on KCl (100) for (a) $t=0$ ps, (b) $t=20$ ps, and (c) $t=40$ ps.

physical origin of the melting of surface is roughly explained if one considers the fact that melting is favored by defects,[31] and that the surface is and acts as a huge defect where atoms, especially after deconstruction, are loosely bound to each other. Thus, the nonmelting surface is considered as a well arranged surface, which resists to the temperature effect much more than the bulk.
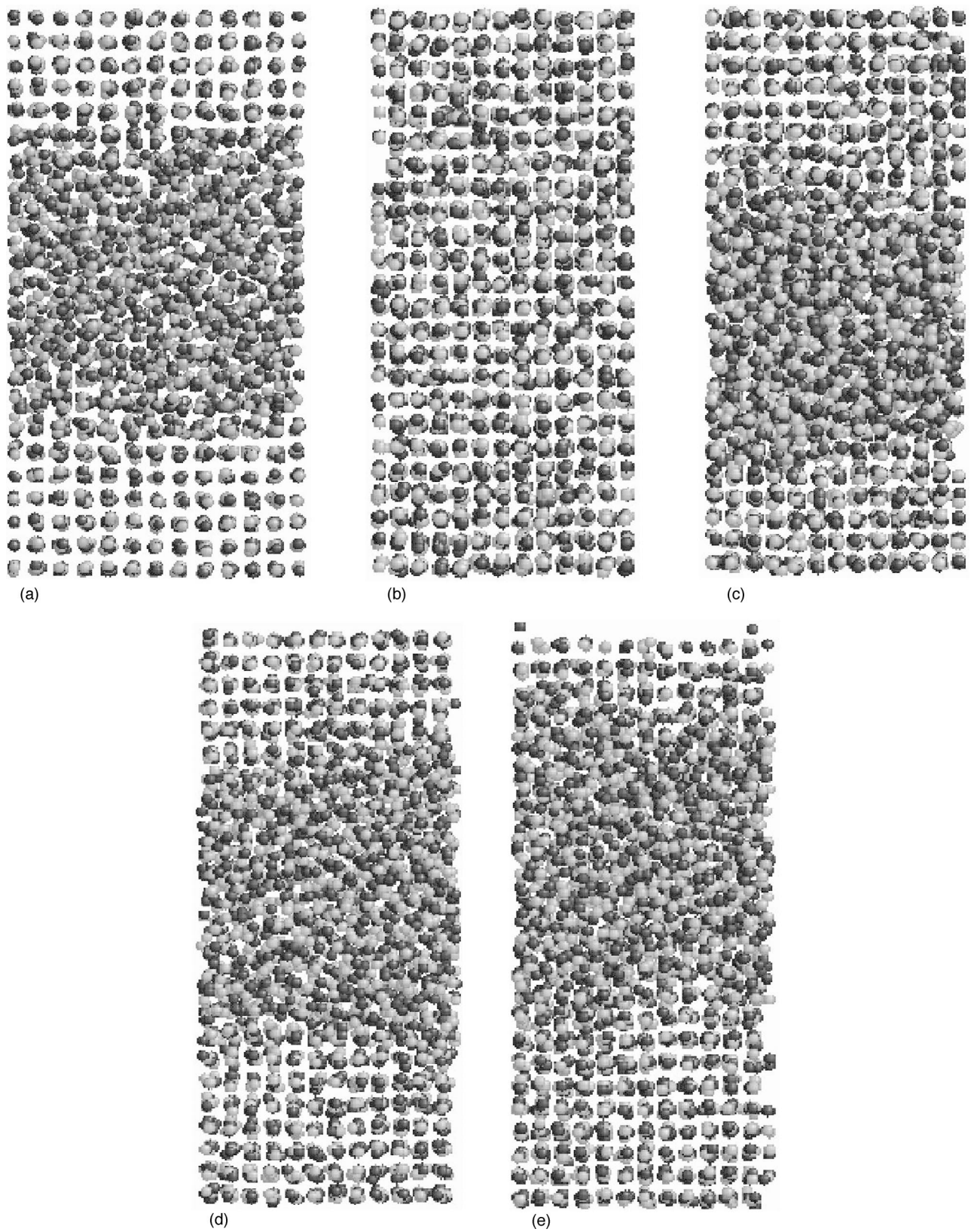
FIG. 6. Freezing effect in KCl (100): (a) initial configuration, (b) $T = 1200$ K, (c) $T = 1330$ K, (d) $T = 1347$ K, (e) $T = 1350$ K.
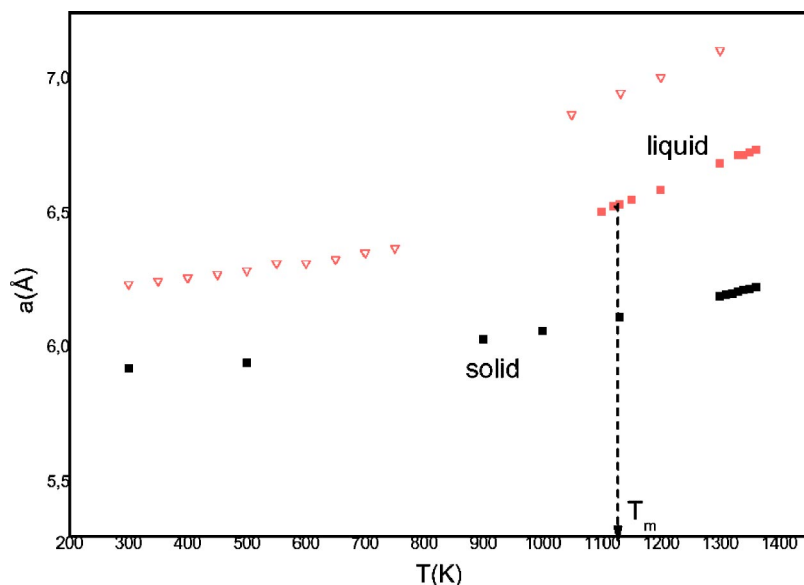
FIG. 7. The lattice parameter versus tempera-ture for the liquid and solid phases (filled squares) compared to the experimental values (empty triangles).

C. Nanodroplet on KCl(100)

Another way to approach the nonmelting problem of the surface is to consider the contact angle between the liquid nanodroplet and the surface of the same material. We pre-pared a crystalline slab containing 7840 atoms, 5 atomic planes thick $[14 \times 14 \times 5 \ (KCl)_4$ conventional cubic cells]. The slab was gradually heated up to the bulk melting point, keeping two atomic layers rigidly fixed at the bottom of the slab. Separately we prepared a small KCl cluster consisting of 500 K and 500 Cl molecular units, by adding a vacuum of 100 Å in the three dimensions directions. The system was overheated sufficiently to have it fully liquid and completely equilibrated. The size of the cluster was chosen to be large enough to yield after melting a near-spherical drop and also a well defined shape when the drop is deposited on the surface of the slab. By deposing the drop on the nonmelting (100) KCl surface, we can learn about its wetting behavior. In Fig. 4, we give a plot showing a general geometry of the shape of a drop melt onto a nonmelting surface of the same material. The two interfaces separating solid and liquid (SL) and liquid and vapor (LV) are assumed to be spherical with radii R_{SL} and R_{LV} and contact angles θ_{SL} and θ_{LV}, respectively. When deposited on the nonmelting KCl (100) face, it does not dif-fuse away, but rather settles down with well-defined angle θ_m. Figure 5 shows three significant steps of the simulation procedure at 0 ps [Fig. 5(a)], at 20 ps [Fig. 5(b)], and after equilibration at 40 ps [Fig. 5(c)].

The determination of the wetting angle θ_{LV} is done as follows: after the equilibration of the system (substrate +droplet), the atomic positions of the 10 last configurations are plotted in cylindrical coordinates. Then, for each configu-ration and from the profile of the droplet, the center position and the radius of a portion of a sphere are determined. θ_{LV} follows directly by a simple geometry from these two quan-tities. For each configuration, we extract θ_{LV} and then θ_m is the mean over the 10 configurations. We can thus extract $\theta_m = 47° \pm 5°$, which is in agreement with the experimental value $\theta_m = 49°$.[22]

The value of the wetting angle can also be calculated using the following equation:[28]

$$\cos \theta_m = 1 - \frac{\Delta \gamma_\infty}{\gamma_{LV}} \qquad (2)$$

with

$$\Delta \gamma_\infty = \left(\frac{T_i}{T_m} - 1 \right) \frac{L_{\rho s}}{\gamma_{LV}}. \qquad (3)$$

s is the thickness of the KCl monolayer, L is the latent-heat of melting and ρ is the crystal density. For KCl, $\gamma_{LV} = 100.2 \pm 0.6$ erg/cm²,[38] $\rho = 1.988$ g/cm³,[39] $L = 2.32 \times 10^9$ erg/g,[39] $s = 6.20$ A. Our calculated value corresponds to $T_i/T_m = 0.19$; consequently, $\theta_m = 51°$, which is the same range of the value obtained from our nanodroplet simulation. From the contact angle result it is understood that if the surface is melting, then the droplet should be completely absorbed. In our case, only a partial absorption appears which means that the surface is nonmelting and confirms again our result pre-sented in the previous section.

D. Surface freezing simulation

In order to investigate the freezing behavior in KCl (100), we adopt a supercell of 24 layers with two free surfaces in which we have fixed as solid 6 layers in the top and 6 layers in the bottom, as shown in Fig. 6(a). The 12 layers in the middle have been carried at high temperature over the bulk melting point in order to have this part liquid. From the following simulations, we aim to know the temperature (the freezing one) for which the initial configuration (solid layers float on the liquid) remains the same after equilibrating the system. In order to achieve this, we have run several calcu-lations for 500 ps at $T = 1200$ K [Fig. 6(b)], 1330 K [Fig. 6(c)], 1347 K [Fig. 6(d)], and 1350 K [Fig. 6(e)], where we attributed the same temperature for the entire system. For the first case, at 1200 K, the atoms in the liquid part enter in interaction with the solid one, loose their kinetic energy, and

as a consequence a sudden decrease of temperature of the liquid part happens which leads to a crystallization of this part, as shown in Fig. 6(b). Then going gradually up to 1330 K, we notice a stabilization of the liquid part with 13 solid layers (5 layers in the top and 8 layers in the bottom). This situation is the same for $T=1347$ K, in which 12 solid layers (5 layers in the top and 7 layers in the bottom) float on the liquid. For the last case, at $T=1350$ K, the number of solid layers decreases, and we obtain after equilibration a system with a liquid part much more pronounced than the solid one. We may conclude that KCl could have a freezing effect in a temperature range from $T=1330$ K to 1347 K. This phenomenon is observed for alkane and several of their derivatives.[40–42] In alkanes, the surface-frozen layer is one molecule thick for chain lengths $16 \leqslant n \leqslant 30$. In our case, we think that this is strongly related to the solid and liquid densities of KCl.

In Fig. 7, we plot the variation of the lattice parameter with temperature compared to experimental measurements,[43] which reflects the variation of the molar fraction. From this figure we can see the important jump between solid and liquid phases (20%) which is also related to the densities of the two states solid (1.988 g/cm^3) and liquid (1.585 g/cm^3). This peculiarity could be behind the unexpected freezing behavior in the surface of this material, since the liquid needs a considerably important energetic effort to be stabilized in a crystal structure.

IV. CONCLUSION

A molecular dynamics study of thermodynamic properties of KCl (100) including nonmelting, wetting, and freezing behaviors has been carried out using a Fumi-Tosi potential. Ewald summation was applied to evaluate the troublesome long-range interactions in this system. The good agreement found for the calculated bulk melting temperature and the experimental one confirms the reliability of the potential model chosen. Our results mainly show a highly ordered surface even at elevated temperature and a droplet stability and solidifications, which is in favorable agreement with the experimental data. We have finally predicted the freezing behavior and explained this phenomenon by the huge difference of the molar fraction between solid and liquid states.

ACKNOWLEDGMENTS

*Present address: Max-Planck-Institut für Metallforschung, Heisenbergstraße 3, D-70569 Stuttgart, Germany. Email address: zaoui@marvin.mpi-stuttgart.mpg.de

†Present address: Max-Planck-Institut für Metallforschung, Heisenbergstraße 3, D-70569 Stuttgart, Germany.

[1] M. Faraday, *Faraday's Diary* (Bell and Sons, London, 1933).

[2] I. N. Stranski, Z. Phys. **119**, 22 (1942).

[3] J. Frenkel, *Kinetic Theory of Liquids* (Clarendon, Oxford, 1946).

[4] J. W. Frenken and J. F. van der Veen, Phys. Rev. Lett. **54**, 134 (1985).

[5] J. W. Frenken, P. M. J. Marée, and J. F. van der Veen, Phys. Rev. B **34**, 7506 (1986).

[6] A. W. Denier van der Gon, R. J. Smith, J. M. Gay, D. J. O'Connor, and J. F. van der Veen, Surf. Sci. **227**, 143 (1990).

[7] J. R. Morris, C. Z. Wang, K. M. Ho, and C. T. Chan, Phys. Rev. B **49**, 3109 (1994).

[8] E. Saiz, A. P. Tomsia, and R. M. Cannon, Scr. Mater. **44**, 159 (2001).

[9] E. Saiz, R. M. Cannon, and A. P. Tomsia, Acta Mater. **48**, 4449 (2000).

[10] E. Saiz, R. M. Cannon, and A. P. Tomsia, Acta Mater. **47**, 4209 (1999).

[11] R. E. Allen, F. W. De Wette, and A. Rahman, Phys. Rev. **179**, 887 (1969).

[12] J. Q. Broughton and L. V. Woodcock, J. Phys. C **11**, 2743 (1978).

[13] J. Q. Broughton and G. H. Gilmer, J. Chem. Phys. **79**, 5105 (1983); **79**, 5119 (1983).

[14] D. M. Zhu and J. G. Dash, Phys. Rev. Lett. **57**, 2959 (1986).

[15] H. M. van Pinxteren and J. W. M. Frenken, Europhys. Lett. **21**, 43 (1993).

[16] H. M. van Pinxteren, B. Pluis, and J. W. M. Frenken, Phys. Rev. B **49**, 13798 (1994).

[17] H. M. van Pinxteren, Ph.D. thesis, University of Amsterdam, 1994.

[18] K. D. Stock and B. Grosser, J. Cryst. Growth **50**, 485 (1980).

[19] K. D. Stock, Surf. Sci. **91**, 655 (1980).

[20] A. Pavlovska, K. Faulian, and E. Bauer, Surf. Sci. **221**, 233 (1989).

[21] J. C. Heyraud, J. J. Métois, and J. M. Bermond, J. Cryst. Growth **98**, 355 (1989).

[22] G. Grange, R. Landers, and B. Mutaftschiev, Surf. Sci. **54**, 445 (1976).

[23] F. G. Fumi and M. P. Tosi, J. Phys. Chem. Solids **25**, 31 (1964).

[24] M. J. L. Sangster and M. Dixon, Adv. Phys. **23**, 247 (1976).

[25] M. A. Allenand and D. J. Tildesley, *Computer Simulation of Liquids* (Oxford Science, Oxford, 1987).

[26] L. V. Woodcock, Chem. Phys. Lett. **10**, 257 (1971).

[27] F. Ercolessi, O. Tomagnini, S. Iarlori, and E. Tosatti, in *Nanosciences and Manipulation of Atoms Under High Fields and Temperatures: Applications*, edited by Vu Thien Binh, N. Garcia, and K. Dransfeld (Kluwer, Dordrecht, 1993), p. 185.

[28] F. Di Tolla, F. Ercolessi, and E. Tosatti, Phys. Rev. Lett. **74**, 3201 (1995).

[29] A. Vijay and T. S. Verma, Physica B **291**, 373 (2000), and references therein.

[30] F. Di Tolla, thesis, 1996.

[31] R. M. Cotterill, E. J. Jensen, W. D. Kristensen, in *Anharmonic Lattices, Structural Transitions and Melting*, edited by T. Riste (Noordhooff, Leiden, 1974).

[32] P. Stoltze, J. K. Norskov, and U. Landman, Phys. Rev. Lett. **61**,

440 (1988).

[33] E. T. Chen, R. N. Barnett, and U. Landmann, Phys. Rev. B **41**, 439 (1990).

[34] R. N. Barnett and U. Landmann, Phys. Rev. B **44**, 3226 (1991).

[35] P. Carnevali, F. Ercolessi, and E. Tosatti, Phys. Rev. B **36**, 6701 (1987).

[36] B. Pluis, A. W. Denier van der Gon, J. W. M. Frenken, and J. F. van der Veen, Phys. Rev. Lett. **59**, 2678 (1987).

[37] A. W. Denier van der Gon, R. J. Smith, J. M. Gaz, D. J. O'Connor, and J. F. can der Veen, Surf. Sci. **227**, 143 (1990).

[38] G. Grange, R. Landers, and B. Mutaftschiev, J. Cryst. Growth **49**, 343 (1980).

[39] L. Batten, C. Carbno, P. Letkeman, T. Myers, M. Tsatsomeros, and S. Yam, Potash Corporation of Saskatchewan.

[40] J. C. Earnshaw and C. J. Hughes, Phys. Rev. A **46**, R4494 (1992).

[41] X. Z. Wu, E. B. Sirota, S. K. Sinha, B. M. Ocko, and M. Deutsch, Phys. Rev. Lett. **70**, 958 (1993).

[42] X. Z. Wu, B. M. Ocko, E. B. Sirota, S. K. Sinha, M. Deutsch, B. H. Cao, and M. W. Kim, Science **261**, 1018 (1993).

[43] G. J. Janz and R. D. Reeves, *Molten-Salt Electrolytes—Transport Properties, Advances in Electrochemistry and Electrochemical Engineering*, edited by Delahay and C. W. Tobias (Wiley-Interscience, New York, 1961–1984, 1967), Vol. 5.